TECHNICAL PAPER

Application of RCGA-ANN approach for modeling kerf width and surface roughness in CO$_2$ laser cutting of mild steel

Miloš Madić · Miroslav Radovanović

Abstract This paper presents an artificial intelligence approach for the development of predictive models for a CO$_2$ laser cutting of mild steel by using artificial neural networks (ANNs) and real coded genetic algorithm (RCGA). Laser cutting experiment, conducted according to Taguchi's experimental design using L_{25} orthogonal array, provided a set of data for the development of ANN models for the prediction of the kerf width and surface roughness. Both ANN models considered cutting speed, laser power, and assist gas pressure as input parameters. Considering the disadvantages of the back propagation, the RCGA was applied for training of the ANNs. Statistical results indicate good correlation between the experimental results and ANN predictions, which confirms the validity of the applied approach. Finally, using the developed models, the combined effects of input process parameters on the quality characteristics were studied.

Keywords Carbon dioxide (CO$_2$) laser cutting · Artificial neural networks · Modeling · Kerf width · Surface roughness · Real coded genetic algorithm

List of symbols

$\mathbf{B}$	Bias matrix of hidden neurons
b_{ok}	Bias of output neuron
d	Desired (target) value
E	Fitness function
F	Transfer function in hidden layer
g	Transfer function in output layer
k	Number of output neurons
K_w	Kerf width, mm
m	Number of hidden neurons
m_{up}	Upper limit of number of hidden neurons
n	Number of input neurons
N_{tr}	Number of data for training
N_{ts}	Number of data for testing
p	Assist gas pressure, bar
P	Laser power, W
R	Correlation coefficient
R_a	Average surface roughness, µm
T	Total number of weights and biases
v	Cutting speed, mm/min
$\mathbf{V}$	Weight matrix between input and hidden layer
$\mathbf{W}$	Weight matrix between hidden and output layer
x_{min}	Minimal value of variable
x_{min}	Maximal value of variable
x^n	Normalized value for variable
$\mathbf{X}$	Vector of input parameters
$\hat{y}$	ANN prediction

M. Madić (✉) · M. Radovanović
University of Niš, Faculty of Mechanical Engineering,
A. Medvedeva 14, 18000 Niš, Serbia
e-mail: madic@masfak.ni.ac.rs

M. Radovanović
e-mail: mirado@masfak.ni.ac.rs

1 Introduction

Among various advanced machining processes, laser cutting is one of the most widely used thermal-based processes applied for processing a wide range of materials. Laser cutting technology finds many applications in various manufacturing industries due to its convenience of operation, high precision, small heat-affected zone, minimum deformity [24], low cost, high quality of end product [19], high processing speed, and low waste [25]. Additionally, as a

noncontact, it is well suited for advanced engineering materials, such as difficult-to-cut materials, brittle materials, electric and non-electric conductors, and soft and thin materials[6]. Numerous advantages and possibilities of laser cutting technology motivated considerable theoretical and experimental research aimed at better understanding of the laser cutting process. Comprehensive review papers about laser cutting are available [7, 8, 16].

The laser cutting process is characterized by a number of controllable and uncontrollable process parameters and their interactions, which in turn determine the efficiency of the whole process in terms of productivity, quality, and costs. Maximization of productivity and quality along with cost minimization are of particular interest to manufacturers. Each of these goals often requires "optimal" selection of cutting parameter settings. With a limited theoretical and practical background to assist in the systematic selection, these parameters are usually set by previous experience in time consuming trial and error procedure. Consequently, it is of great importance to exactly quantify the relationships between laser cutting parameters and cutting performances through mathematical modeling. Different methodologies were employed for modeling of laser cutting, such as analytical methods, statistical experimental design, and artificial intelligence (AI)-based methods. Few researchers concentrated on modeling and optimization of laser cutting through AI-based techniques, such as artificial neural networks (ANNs) [1, 4, 19, 26] and fuzzy logic [22]. Chen et al. [6] presented an approach for optimization of laser cutting process with multiple performance characteristics based on Taguchi method and grey relational analysis.

ANNs as one of the most used AI methods have proved to be one of the most powerful modeling tools based on the statistical approach. The ability of ANN to capture any complex input–output relationships from limited data is very valuable in manufacturing processes where huge experimental data for the process modeling are difficult and expensive to obtain [13]. In addition, they are more efficient modeling tool when compared with other classical prediction methods [2]. They are especially suitable in situations where mathematical formulae and prior knowledge on the functional relationship between process parameters are unknown. Among different ANN types, single hidden layer back propagation (BP) ANN is considered as most popular variant of multilayer feed forward ANN for modeling of complex nonlinear relationships between multiple input and the output variables [4]. The most common training algorithm for ANNs is the BP algorithm and its variants because it is stable and easy to implement. Conventional BP and faster algorithms like Levenberg–Marquardt have been already used for input/output modeling in the field of laser cutting [19, 26]. However, because ANNs generate complex error surfaces with multiple local optima, even for simple

functions being estimated, BP tends to become trapped in local solutions that are not global [9]. In addition, the basic BP algorithm is often very slow to converge in real practice [10]. Considering the disadvantages of the BP, researchers observed that genetic algorithms (GAs) might prevent ANN from falling into a local optimum during training [9, 14]. Gupta and Sexton [9] showed that the GA is superior to the BP in effectiveness, ease of use, and efficiency for training. Furthermore, as noted by [3], real coding is the most suitable coding for continuous domains, and it is beneficial to use real coded genetic algorithm (RCGA) for the ANN training.

As the present study deals with relatively small number data obtained from Taguchi's experimental design, training of ANNs using the RCGA is thought to be an appropriate algorithm for the purpose of developing accurate and robust ANN models for the prediction of cut quality in CO_2 laser cutting.

2 Modeling methodology

Relationship between laser cutting parameters (cutting speed, laser power, and assist gas pressure) and the output parameters (kerf width and surface roughness) was obtained from the ANN models. Two ANN models with the same architecture were designed for each of the output parameters. Experimental results, obtained from Taguchi's experimental design, were used for developing predictive models. The experimental data were randomly divided into a data subset for the ANN training ($N_{tr} = 20$), and data subset for testing the prediction accuracy of the ANN models ($N_{ts} = 5$). Among the various kinds of ANN models, feed-forward multilayer perceptron (MLP) was selected due to its robustness and ability to approximate any nonlinear relationship. To overcome the local convergence problem of the BP, RCGA was chosen as an appropriate method to be used for the ANN training. The aim of RCGA is to simultaneously search for the near optimal set of weights and biases of the ANNs so that ANNs are able to accurately model the CO_2 laser cutting process.

3 Experimental setup

Experiment trials were conducted using a 2.2 kW CO_2 ByVention 3015 laser cutting machine provided by Bystronic Inc. The cuts were performed with a Gaussian distribution beam mode (TEM_{00}) on 2-mm-thick commercial mild steel sheet. Oxygen gas with a purity of 99.95 % was employed as an assist gas. The laser beam was focused on the surface of the samples using a focusing lens with a focal length of 5 in. (127 mm). The conical shape nozzle

Table 1 Laser cutting parameters and their levels

Cutting parameter	Unit	Level				
		1	2	3	4	5
Cutting speed, v	mm/min	3,000	4,000	5,000	6,000	7,000
Laser power, P	W	700	900	1,100	1,300	1,500
Assist gas pressure, p	bar	3	4	5	6	7

Table 2 Experimental design and results

Trial	V (mm/min)	P (watts)	p (bar)	R_a (µm)	K_w (mm)
1	3,000	700	3	1.487	0.228
2	3,000	900	4	1.290	0.278
3	3,000	1,100	5	2.073	0.293
4	**3,000**	**1,300**	**6**	**2.477**	**0.427**
5	3,000	1,500	7	2.937	0.667
6	4,000	700	4	1.780	0.255
7	4,000	900	5	1.707	0.327
8	**4,000**	**1,100**	**6**	**2.337**	**0.302**
9	4,000	1,300	7	3.307	0.328
10	4,000	1,500	3	1.190	0.330
11	5,000	700	5	2.013	0.303
12	5,000	900	6	2.017	0.288
13	5,000	1,100	7	2.603	0.305
14	**5,000**	**1,300**	**3**	**1.173**	**0.302**
15	5,000	1,500	4	1.380	0.292
16	6,000	700	6	1.660	0.253
17	6,000	900	7	1.710	0.277
18	6,000	1,100	3	0.963	0.273
19	**6,000**	**1,300**	**4**	**1.007**	**0.268**
20	6,000	1,500	4	1.143	0.293
21	7,000	700	7	1.587	0.255
22	7,000	900	3	0.832	0.250
23	7,000	1,100	4	0.903	0.300
24	**7,000**	**1,300**	**5**	**0.88**	**0.275**
25	7,000	1,500	6	1.073	0.312

Bolded rows denote data for ANN

(HK10) with 1-mm nozzle diameter was used. The nozzle–work piece stand-off distance was controlled at 0.7 mm. Focusing lens, focus position, nozzle diameter, nozzle stand-off distance, and sheet thickness were kept constant throughout the experimentation.

In the present experimental study, three input parameters, namely: cutting speed (v), laser power (P), and assist gas pressure (p), were considered. The parameter ranges were varied by about 40 % above and below their normal operating level as recommended by the machine manufacturer (Table 1).

To study the entire experimental region with minimum cost and time of the experiment, Taguchi experimental design was applied. Based on the selected parameters and parameter levels, a design matrix was constructed in accordance with the standard L_{25} Taguchi's orthogonal array (Table 2).

Two cuts, 60-mm length each, were made in every experimental trial. The laser cut quality was assessed by measuring kerf width and surface roughness. Surface roughness on the cut edge was measured in terms of the average surface roughness (R_a) using Surftest SJ-301 (Mitutoyo) profilometer. Cutoff length was 0.8 mm, and evaluation length was 4 mm. Each measurement was taken along the cut at approximately the middle of the thickness, and the measurements were repeated three times to obtain averaged values. The kerf width (K_w) of each cut was measured at three equally distanced locations along the length of cut by means of Eschenbach scaled magnifier ($10\times$) with illumination and digital micrometer (Mitutoyo) with accuracy of 0.01 mm.

4 Kerf width and surface roughness ANN models

4.1 ANNs functioning

The MLP represents fully connected feed-forward network architecture composed of many interconnected neurons grouped into input, hidden, and output layer. The functioning of a three-layer feed-forward ANN with n input neurons, m hidden neurons, and one output neuron can be expressed by the following mathematical relation:

$$\hat{y} = g\left(\sum_m \mathbf{W} \cdot f\left(\sum_n \mathbf{V} \cdot \mathbf{X} + \mathbf{B} \right) + b_{ok} \right) \quad (1)$$

where V and W are weight matrices between input and hidden layer and hidden and output layer, respectively; $\mathbf{B}$ is the bias matrix of hidden neurons; b_{ok} is the bias of output neuron; X is the vector of input parameters; f and g are transfer functions in hidden and output layer, respectively; and $\hat{y}$ is the ANN prediction.

Determining weights and biases, in which the "knowledge" of the ANN is kept, is done during training process where examples (input–output pairs) are presented to the ANN. Training is a continuous process, which is repeated until the differences between predicted and the target (experimental) values are below previously defined threshold. The trained ANN should be tested on selected set of input–output data (testing data) in order to assess its ability to predict and make generalization on the basis of the acquired "knowledge". Finally, the trained and tested ANN can be used for modeling and

prediction of outputs when it is presented with new (original) input data.

4.2 ANNs design

The ANN models were aimed to predict the kerf width (K_w) and average surface roughness (R_a) considering three process parameters, namely: cutting speed (v), laser power (P), and assist gas pressure (p). To this aim, two ANN models were developed:

- Model 1—which relates v, P, p, and K_w, and
- Model 2—which relates v, P, p, and R_a.

In order to increase prediction accuracy, stabilize and enhance ANN training, the input and output data were normalized between −1 and 1 by the following equation:

$$x_i^n = 2 \cdot (x_i - x_{min})/(x_{max} - x_{min}) - 1; \; i = 1, \ldots, n \quad (2)$$

where x_i^n is the normalized value for the variable, and x_{min} and x_{max} are the minimum and maximum of each variable x_i.

Linear transfer function and hyperbolic tangent sigmoid transfer function were used in the output and hidden layer, respectively. These transfer functions were used, since it was assumed that there exists nonlinear relationship between input and output process parameters.

It has been widely reported that ANN with a single hidden layer are able to approximate any arbitrary function to a given accuracy. Therefore, the selection of ANN architecture can be reduced to finding the "optimal" number of hidden neurons. Too few neurons in hidden layer can lead to under-fitting, whereas too many neurons can contribute to over-fitting [13].

For the single hidden layer ANN architecture with n input neurons, m hidden neurons and k output neurons, the total number of weights and biases can be expressed as

$$T = m \cdot (n + k + 1) + k \quad (3)$$

The upper limit of number of hidden neurons can be determined considering that the total number of weights and biases in the ANN does not exceed the number of data for training (N_{tr}). Though the ANN can still be trained, the case is mathematically undetermined [20]. For ANNs with single output neuron ($k = 1$), the upper limit of number of hidden neurons can be determined by

$$m_{up} \leq (N_{tr} - 1)/(n + 2) \quad (4)$$

In order to take full modeling potential of the ANN, the 3-3-1 ANN architecture was selected for both models.

4.3 ANNs training

The ANN models were trained with the RCGA using the available training data. The RCGA itself is not discussed,

and the details are available elsewhere along with numerous examples of applications [3, 5, 15, 18]. A review related to RCGA is also available [11]. Prior to using the RCGA for ANN training, the explicit mathematical model of the 3-3-1 ANN architecture was created using MATLAB package. The aim of the RCGA was to explore the search space to find optimal or near-optimal weights and biases on the ANNs. These include weights between the input layer and the hidden layer, weights between the hidden layer and the output layer, biases of the hidden neurons and bias of the output neuron. Therefore, the optimization problem involved determining of total 16 weight and bias values, that is,

$$\mathbf{V} = \begin{bmatrix} v_{11} & v_{12} & v_{13} \\ v_{21} & v_{22} & v_{23} \\ v_{31} & v_{32} & v_{33} \end{bmatrix};$$

$$\mathbf{W} = \begin{bmatrix} w_1 & w_2 & w_3 \end{bmatrix}; \quad \mathbf{B} = \begin{bmatrix} b_1 & b_2 & b_3 \end{bmatrix}; \quad b_{ok}; \quad (5)$$

The objective of the RCGA application was to approximate connection weights and biases given in Eq. (5) such that to minimize the following fitness function:

$$E = \sum_{i=1}^{N_{tr}} |d_i - \hat{y}_i| \quad (6)$$

where d_i and y_i are the i-th target (experimental) and ANN predicted values, respectively.

Basically, obtaining the best optimal results depends on some features related to the RCGA parameters. Although some general guidelines about such selections exist in relevant literature, it was reported that optimal setting is strongly related to the design problem under consideration [1]. After few trials were conducted, the parameters of the RCGA's for both models were set as shown in Table 3 since with these settings minimum error was observed.

Figure 1 shows the best function value in each generation versus iteration number and convergence of the optimization problem.

After an iterative calculus, the RCGA provided the (near) optimal values for weights ($\mathbf{V}$, $\mathbf{W}$) and biases ($\mathbf{B}$, b_{ok}) for the ANN models (Table 4).

Table 3 RCGA parameter values used for ANN training

RCGA parameters	Value
Population size	20
Selection	Stochastic uniform
Reproduction	Elite count: 2 crossover fraction: 0.9
Crossover function	Scattered
Mutation function	Gaussian

5 Results and discussion

5.1 Prediction performance of the ANN models

Regarding the data normalization, transfer functions used in the ANNs and using the weights and biases from Table 4, one can predict the kerf width and surface roughness using Eq. (1). The prediction performance of the ANN models was examined based on the correlation coefficient between the ANN predictions and the experimental values using both training and testing data. Figure 2a shows good agreement of the results for kerf width and the experimental results given in Table 2. Also, Fig. 2b shows good accuracy of calculation for the surface roughness, compared with the experimental values of the average surface roughness.
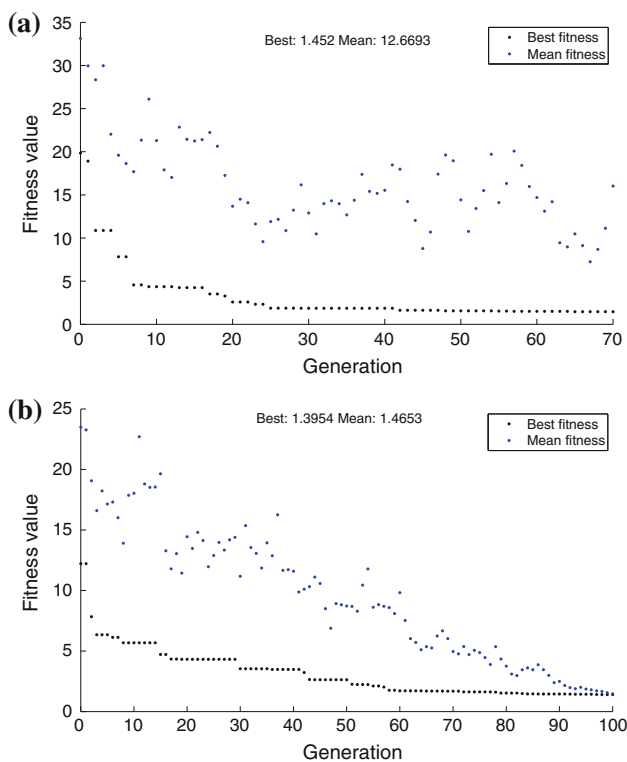

Fig. 1 Plot functions of the best fitness for **a** Model 1 and **b** Model 2

To get a better picture of the ANN models' prediction performance, the statistical methods of correlation coefficient (R) and mean absolute percent error (MAPE) were calculated separately for both training and testing data (Table 5).

The results from Fig. 2 and Table 5 indicate that the developed ANN models can be used for the prediction of the kerf width and surface roughness for arbitrarily chosen values of cutting parameters with good accuracy. Thus, the influence of the cutting parameters on the kerf width and surface roughness can be studied using the developed ANN models. The effects of the cutting parameters were examined at different combinations of input parameters. Kerf width and surface roughness variation are shown in Figs. 3 and 4 with two parameters in interaction, keeping other parameter constant.

5.2 Effects of cutting parameters on the kerf width

As seen from Fig. 3a, the effect of the cutting speed on the kerf width is nonlinear and variable. For assist gas pressure below 5 bar, in the first stage the kerf width increases with the increase of the cutting speed, but after a certain limit, the increase of the cutting speed adversely affects the kerf width, and the kerf width decreases with the increase of the cutting speed. Laser cutting is a complicated process because melting and evaporation of material take place simultaneously under laser beam power and exothermal reaction by the action of oxygen. For a given laser power level, reducing the laser cutting speed increases the duration for which the high temperature oxidation reaction takes place at the workpiece surface. In this case, the influence of the assist gas pressure is obvious, i.e., the combination of high assist gas pressure with low cutting speed enhances the energy coupling at the workpiece surface and increases the kerf width considerably (Fig. 3a). In general, it was observed that a decrease in the kerf width occurs with an increase in the cutting speed. These results are in agreement with those reported in references [17, 23, 25]. This is due to the fact that an increase in cutting speed reduces the rate of energy transfer from the laser source to
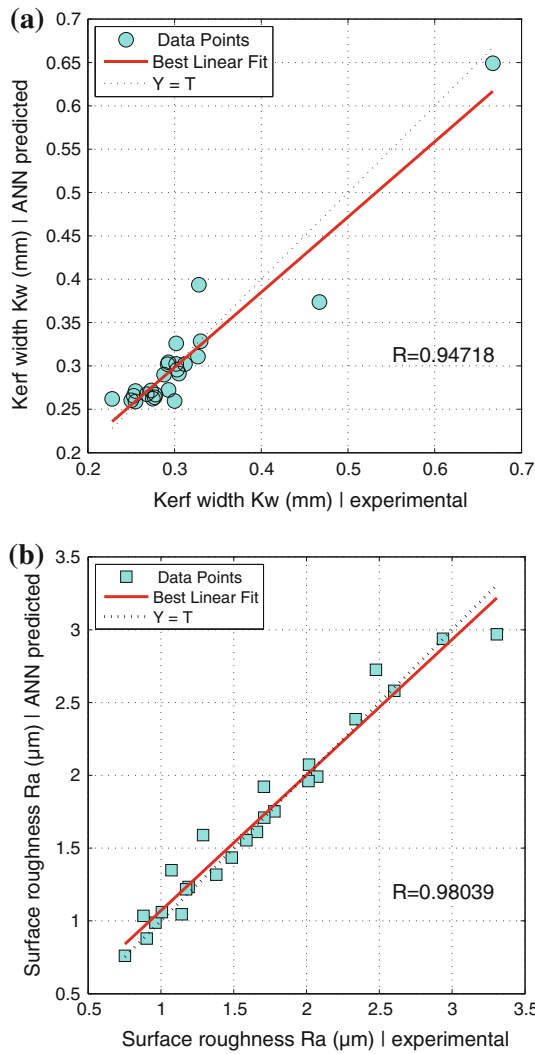
Table 4 Experimental design and results

ANN	V			W	B	b_{ok}
Model 1	2.1337	0.2766	0.4269	−0.1730	0.1000	0.5490
	0.3967	−1.5386	−1.0616	−1.4032	2.9569	–
	2.4180	1.3974	1.3620	0.1638	2.5242	–
Model 2	0.0699	−0.6479	1.2718	0.3999	0.1759	−0.1607
	1.2323	−1.2739	−1.8049	−0.3773	1.7168	–
	3.5479	−0.3268	0.3860	−0.2466	−1.4582	–

108

J Braz. Soc. Mech. Sci. Eng. (2013) 35:103–110

Fig. 2 Comparison of measured and predicted values for **a** K_w and **b** R_a

Table 5 Experimental design and results

ANN	Training data		Testing data	
	R	MAPE	R	MAPE
Model 1	0.968	5.38	0.924	5.07
Model 2	0.979	6.13	0.995	7.79

the workpiece material [23] which results in decrease in side burning [21].

As seen from Fig. 3b, generally, increasing the laser power enhances the kerf width size. Moreover, as the cutting speed increases the kerf width reduces which is particularly evident at higher laser power levels. When comparing the present predictions with the previous findings [23, 25], it can be noted that both results agree. For cutting speed above 5,000 mm/min, the kerf width is decreasing slowly until a certain limit with the increase of
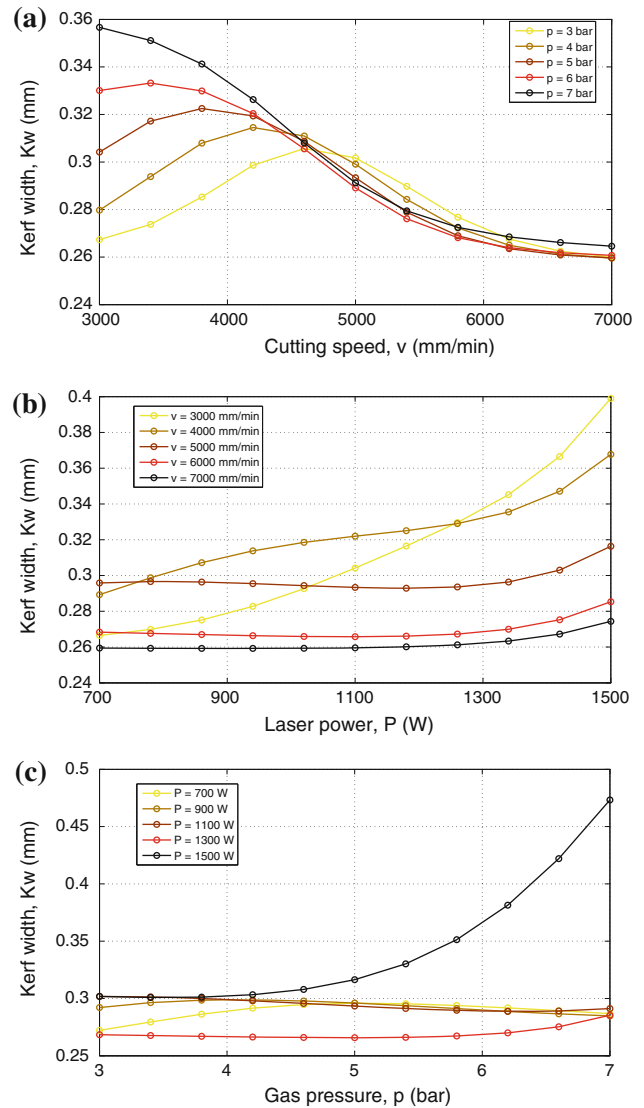

Fig. 3 Variation of kerf width with **a** cutting speed and assist gas pressure, **b** laser power and cutting speed, and **c** assist gas pressure and laser power

the laser power but it begins increasing with the increase of the laser power after about 1,200 W. On the other side, for lower cutting speeds, the kerf width is increasing rapidly. These findings are in agreement with previously reported [25]. At higher laser power levels, the ignition zone is expected to be wider because of the higher heat input [17]. As the interaction effect of the laser power and the cutting speed determines the amount of heat that enters the workpiece during processing, combination of the lowest laser power level and the highest cutting speed level resulted in the lower heat input during machining and consequently, the lowest kerf width was observed.

For cutting speed of 5,000 mm/min, the increase in oxygen gas pressure produces small changes in the kerf width (Fig. 3c). However, the interaction effect of the
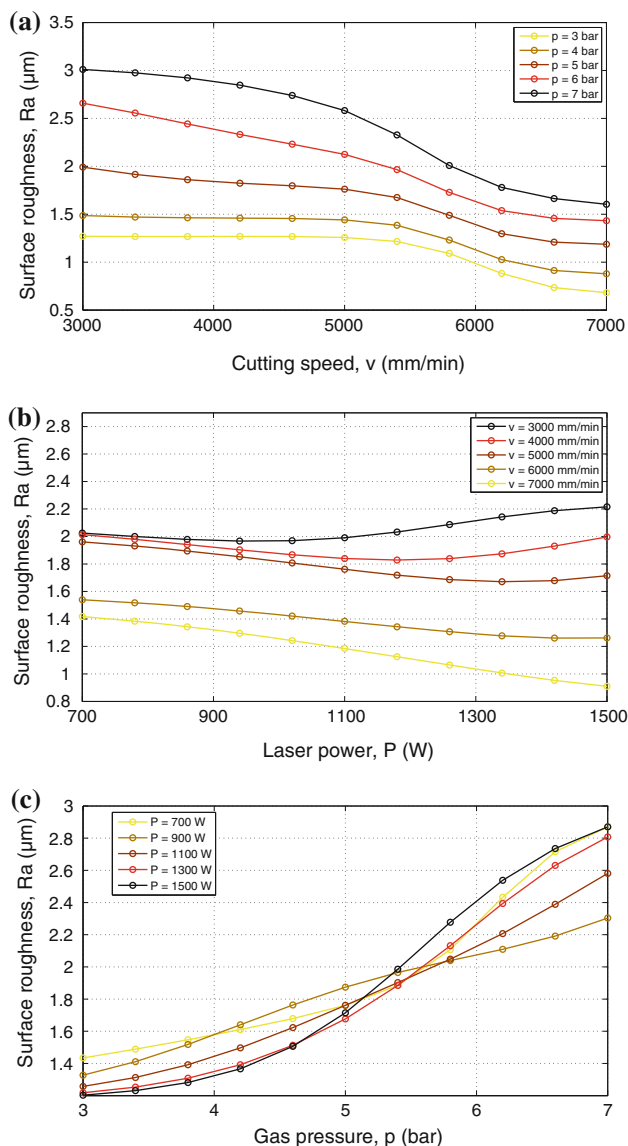
J Braz. Soc. Mech. Sci. Eng. (2013) 35:103–110

109

Fig. 4 Variation of surface roughness with **a** cutting speed and assist gas pressure, **b** laser power and cutting speed, and **c** assist gas pressure and laser power

5.3 Effects of cutting parameters on the surface roughness

As seen from Fig. 4a, for laser power of 1100 W, an increase in the cutting speed decreases the surface roughness for assist gas pressures ranging from 3 to 7 bar. This is due to the fact that as the cutting speed increases, the interaction time between the laser beam and workpiece material decreases, hence the thermal energy available at the workpiece surface decreases, which results in minimum side burning of the cut edge. On the other hand, increasing the heat input (low cutting speed and high laser power) increases the kerf width and surface roughness.

An increase in laser power improves surface roughness in the 700–1,000 W laser power range (Fig. 4b). This is because laser cutting is less stable at low power levels [17, 21]. Above this range, the effect of the laser power is variable depending on the cutting speed.

At lower cutting speeds, there is sufficient time for heat diffusion and melting wider grooves which cause surface deterioration. Actually, for a given cutting speed and assist gas pressure, there exists an optimum laser power which provides good surface finish.

An increase in the assist gas pressure increases the surface roughness, and this functional dependence follows the same trend apart from the values of the laser power (Fig. 4c). By increasing the oxygen pressure, the exothermic-induced burning of the cut surface is increased and also drag force is enhanced which results in higher surface roughness.

It should be noted that the variations of the kerf width and surface roughness with laser cutting parameters were not consistent probably because of the interaction effects between the laser cutting parameters and/or presence of impurities and inclusions (pockets of phosphorus and sulfur) within mild steel workpiece.

With respect to the various combinations of laser cutting parameters used in the experimental design, the dross formation has been observed. In high-speed CO_2 laser cutting of mild steel (experimental trials 21, 22 and 23 in Table 2), the different combinations of the laser power and assist gas pressure levels resulted in dross formation. This was also observed when using low cutting speeds (experimental trials 4 and 5 in Table 2) wherein high laser power and increased oxygen pressure led to excessive exothermal reaction resulting in wide irregular kerf and dross formation.

For most of the cutting conditions performed in the study, the top kerf width was larger than the bottom kerf width indicating the tapered nature of CO_2 laser cutting as caused by the loss of laser beam intensity and gas pressure across the thickness of the cut.

assist gas pressure and the laser power of 1,500 W results in continual increase of the kerf width. When the high power laser beam is absorbed by the workpiece material, it results in solid-state heating, melting and evaporation of the workpiece material. The melted and the evaporated material together with the oxygen from the impinging gas initiate a high temperature exothermic reaction [25]. This ionizes the evaporation front slightly and generates a partially ionized surface plasma [12] which acts as a heat source, enlarging the size of the melt in the kerf. This effect was particularly pronounced when using high laser power (1,500 W) and high assist gas pressure (7 bar) when wide kerf is produced (Fig. 3c).

110

J Braz. Soc. Mech. Sci. Eng. (2013) 35:103–110

6 Conclusions

This paper proposes an approach for the development of predictive models for a CO_2 laser cutting using the ANN models trained by the RCGA. Experimental results from the Taguchi's experimental design, where three cutting parameters (cutting speed, laser power and assist gas pressure) were arranged, were used to develop ANN prediction models for the kerf width and surface roughness. The ANN models' prediction results were compared with the experimental results and were statistically assessed. Considering the ANN model architectures and available data for training, it can be concluded that the RCGA offers reliable ANN training along with good prediction results of ANNs. In addition, fast and easy implementation in MATLAB software package makes applied approach an alternative that can be effectively used in the prediction of CO_2 laser cutting process. It should be noted that the prediction performance may be more enhanced by exploiting the full potential of the RCGA through fine tuning of the RCGA parameters.

It can be concluded that the proposed approach can be efficiently used for the mathematical modeling and analysis of the effects of process parameters on the cut quality characteristics with the ultimate aim of better understanding of the CO_2 laser cutting process.

The practical application of the developed models derived from the study can provide a fundamental foundation for the manufacturers using laser cutting technology. Integration of the developed models with an optimization method will lead to improvement of product quality via appropriate selection of the process parameters.

References

1. Adineh VR, Aghanajafi C, Dehghan GH, Jelvani S (2008) Optimization of the operational parameters in a fast axial flow CW CO_2 laser using artificial neural networks and genetic algorithms. Opt Laser Technol 40(8):1000–1007
2. Aguiar PR, Paula WCF, Bianchi EC, Ulson JAC, Cruz CED (2010) Analysis of forecasting capabilities of ground surfaces valuation using artificial neural networks. J Braz Soc Mech Sci Eng 32(2):146–153
3. Blanco A, Delgado M, Pegalajar MC (2001) A real-coded genetic algorithm for training recurrent neural networks. Neural Networks 14(1):93–105
4. Chaki S, Ghosal S (2011) Application of an optimized SA-ANN hybrid model for parametric modeling and optimization of LASOX cutting of mild steel. Prod Eng Res Devel 5(3):251–262
5. Changyu S, Lixia W, Qian L (2007) Optimization of injection molding process parameters using combination of artificial neural network and genetic algorithm method. J Mater Process Technol 183(2–3):412–418
6. Chen MF, Ho YS, Hsiao WT, Wu TH, Tseng SH, Huang KC (2011) Optimized laser cutting on light guide plates using grey relational analysis. Opt Lasers Eng 49(2):222–228
7. Dubey AK, Yadava V (2008) Laser beam machining—a review. Int J Mach Tools Manuf 48(6):609–628
8. Dutta Majumdar J, Manna I (2003) Laser processing of materials. Sadhana 28(3–4):495–562
9. Gupta JND, Sexton RS (1999) Comparing backpropagation with a genetic algorithm for neural network training. Omega 27(6):679–684
10. Hao W, Zhu X, Li X, Turyagyenda G (2006) Prediction of cutting force for self-propelled rotary tool using artificial neural networks. J Mater Process Technol 180(1–3):23–29
11. Herrera F, Lozano M, Verdegay JL (1998) Tackling real-coded genetic algorithms: operators and tools for behavioural analysis. Artif Intell Rev 12(4):265–319
12. Yilbas BS, Yilbas Z (1988) Effects of plasma on CO_2 laser cutting quality. Opt Lasers Eng 9(1):1–12
13. Karnik SR, Gaitonde VN, Campos Rubio J, Esteves Correia A, Abrão AM, Paulo Davim J (2008) Delamination analysis in high speed drilling of carbon fiber reinforced plastics (CFRP) using artificial neural network model. Mater Des 29(9):1768–1776
14. Kim K, Han I (2000) Genetic algorithms approach to feature discretization in artificial neural networks for the prediction of stock price index. Expert Syst Appl 19(2):125–132
15. Kim SS, Kim IH, Mani V, Kim HJ (2008) Real-coded genetic algorithm for machining condition optimization. Int J Adv Manuf Technol 38(9–10):884–895
16. Meijer J (2004) Laser beam machining (lbm), state of the art and new opportunities. J Mater Process Technol 149(1–3):2–17
17. Rajaram N, Sheikh-Ahmad J, Cheraghi SH (2003) CO_2 laser cut quality of 4130 steel. Int J Mach Tools Manuf 43(4):351–358
18. Rolnik VP, Seleghim PJ (2006) A specialized genetic algorithm for the electrical impedance tomography of two-phase flows. J Braz Soc Mech Sci Eng 28(4):378–389
19. Tsai MJ, Li CH, Chen CC (2008) Optimal laser-cutting parameters for qfn packages by utilizing artificial neural networks and genetic algorithm. J Mater Process Technol 208(1–3):270–283
20. Sha W, Edwards KL (2007) The use of artificial neural networks in materials science based research. Mater Des 28(6):1747–1752
21. Sundar M, Nath AK, Bandyopadhyay DK, Chaudhuri SP, Dey PK, Misra D (2009) Effect of process parameters on the cutting quality in LASOX cutting of mild steel. Int J Adv Manuf Technol 40(9–10):865–874
22. Syn CZ, Mokhtar M, Feng CJ, Manurung YHP (2011) Approach to prediction of laser cutting quality by employing fuzzy expert system. Expert Syst Appl 38(6):7558–7568
23. Uslan I (2005) CO_2 laser cutting: kerf width variation during cutting. Proc Inst Mech Eng Part B J Eng Manuf 219(8):571–577
24. Yang CB, Deng CS, Chiang HL (2011) Combining the Taguchi method with artificial neural network to construct a prediction model of a CO_2 laser cutting experiment. Int J Adv Manuf Technol. doi:10.1007/s00170-011-3557-2
25. Yilbas BS (2001) Effect of Process Parameters on the Kerf Width during the Laser Cutting Process. Proc Inst Mech Eng Part B J Eng Manuf 215(10):1357–1365
26. Yousef BF, Knopf GK, Bordatchev EV, Nikumb SK (2003) Neural network modelling and analysis of the material removal process during laser machining. Int J Adv Manuf Technol 22(1–2):41–53